JOURNAL OF MATERIALS SCIENCE 7 (1972) 929–938

The effect of Si, Zr, Al and Mo on the structure and strength of Ti martensite

H. M. FLOWER, P. R. SWANN, D. R. F. WEST
Department of Metallurgy, Imperial College of Science and Technology, London, UK

The structure and strength of martensite in "near α" titanium alloys have been studied in the composition range (wt %) up to 10% Zr, 6%, Al, ½% Mo, 2.4% Si. [0001], $\frac{1}{3}\langle 11\bar{2}0\rangle$ dislocations, $\frac{1}{3}\langle 10\bar{1}0\rangle$ stacking faults and approximately $\{10\bar{1}1\}$ twin related martensite plates are found to be common features of the martensite. Martensite "midribs" consist either of finely transformed material between martensite plates, or regions of low dislocation density within martensite plates.

The martensite morphology is related to the alloy composition, changing from "massive" to "plate-like" with increasing solute content. The strength of the martensite is controlled largely by solid solution strengthening.

1. Introduction

α (hcp) titanium has a much better creep resistance than β (bcc) titanium [1] and the "high temperature" titanium alloys are therefore predominantly α and contain only small additions of β stabilizing elements [2]. One important group of alloys contains typically Al and Zr with small quantities of silicon (0.5 wt % max) and molybdenum (~ 0.5% typical). Their heat-treatment involves rapid cooling from the β field to produce α′ martensite followed by "ageing" at, or above, 500° C. The results reported here form part of a study of the relationship between structure and strength in alloys of the Ti-Zr-Al-Mo-Si system. They concern specifically the martensite produced by water quenching from the β field. Selected alloys have been examined with the aim of elucidating the roles played by the elements in the complex commercial alloys. Knowledge of the microstructure provides a basis for the understanding of the changes resulting from ageing prior to elevated temperature service [3].

2. Experimental procedure

The basis materials were sponge titanium and zirconium and high purity silicon, aluminium and molybdenum. The alloys were prepared as 30g "ingots" by arc melting in an argon atmosphere using several remelts to ensure homogeneity. Weight changes resulting from melting were very small (± 0.06%) and the compositions were taken to be those calculated from the weights of the components. The rod-shaped ingots (approx 50 × 10 × 10 mm) were wrapped in molybdenum foil and were solution treated for 24 h at 1200 ± 5° C in argon filled silica tubes; the alloys were then water quenched, the silica being broken on contact with the water to ensure a rapid quench. Specimens were "sliced" from the ingots for hardness testing and microscopy. The alloy compositions were as shown in Table I. In the text alloys are denoted by their approximate composition in wt %: thus Ti 5% Zr 2.9% Al 1% Si is denoted by Ti-5Zr-3Al-1Si.

3. Results

Since the structure and strength of titanium martensite is strongly influenced by oxygen content [4, 5, 6] several melts were made of most of the alloys studied to check for consistency. Also some specimens were solution-treated and water-quenched twice to evaluate the degree of contamination produced by the experimental method. No significant differences were observed in the structure and strength of the different melts or in the specimens given the double solution-treatment. Specimens of unalloyed titanium also retained a hardness of approximately 115 VPN after several melting cycles. It was concluded therefore that the structures and hardness values obtained reflect interstitial level the order of those present in the starting maters

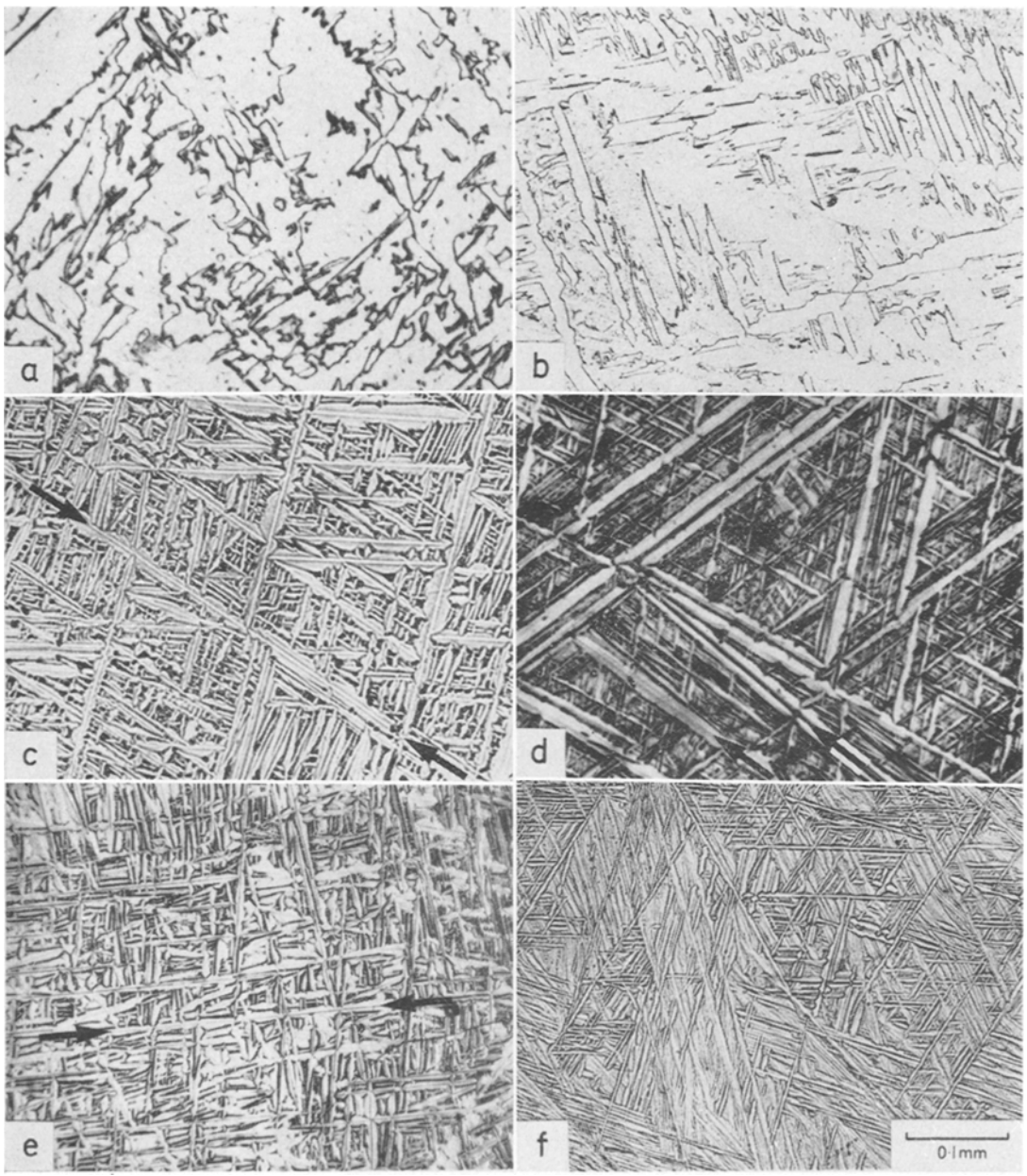

Figure 1 (a) Ti-0.5Si (b) Ti-1Si (c) Ti-2.4Si (d) Ti-5Zr-1Si (e) Ti-5Zr-5Al-1Si (f) IMI 685 type. Light and dark etching midribs are indicated by arrows. Light micrographs.

ials and primarily of the titanium (total interstitial content ~ 0.05 wt %).

3.1. Binary alloys

The series of binary Ti-Si alloys showed that the martensite morphology changes with increase in solute content. In unalloyed titanium the quenched structure, as seen by light microscopy shows serrated-edged grains typical of a "massive martensite"; these are revealed by electron microscopy as bundles (colonies) of plate-shaped crystals, containing dislocations and separated by sub-boundaries. Electron microscopy of the quenched titanium also shows some crystals of approximately equiaxed shape. At a silicon level of 0.5 wt %, the structure

TABLE I Alloy compositions

Ti-Si	0.1, 0.2, 0.5, 0.75, 1.0, 1.5, 2.4 wt % 0.17, 0.3, 0.75, 1.3, 1.7, 2.6, 4.0 at. %
Ti-Zr-Si	5.0 Zr + 0, 0.5, 1.0, 1.5*, Si 2.7 0.85 1.7 2.6 1.0 Zr + 1.5 Si* 0.06 1.8 1.0 Si + 3.0, 10.1 Zr 1.7 1.6 5.5
Ti-Al-Si	5.0 Al + 0, 1.0 Si 8.5 1.6
Ti-Zr-Si-Al	5 Zr 1.0 Si + 1.0, 2.9, 5.0 Al 2.6 1.7 1.7 5.1 8.7
Ti-Al-Zr-Mo-Si	6.0 Al 5.0 Zr 0.5 Mo 0.5 Si
(IMI 685 type)	10.4 2.6 0.25 0.8

*Solution treatment 20 h/1300°C to ensure complete solution of silicon.

consists predominantly of massive martensite, but some relatively large plates are seen by light microscopy (Fig. 1a). Examination of the massive martensite by electron microscopy shows approximately parallel sub-boundaries. Although these sub-boundaries are irregular, the trace of the "average" sub-boundary plane was found to lie within 10° of a {3 3 4} β trace (assuming Burgers α/β orientation relationship applies).

It was noted that in structures containing a mixture of massive colonies and conventional martensite plates, the sub-boundaries in the colonies often ran parallel to the habit planes of the neighbouring plates. The large conventional martensite plates seen by light microscopy, were found by transmission electron microscopy to contain either a uniform distribution of dislocations or parallel arrays of low angle sub-boundaries. In Ti-1Si alloy these large plates occupy the greater proportion of the structure (Fig. 1b). With further increase in silicon content the massive colonies are progressively replaced by individual parallel-sided plates, surrounded by variants of differing orientation; these plates eventually develop a lenticular morphology (Fig. 1c). No retained β or silicide precipitate particles were detected.

A number of selected area diffraction patterns were taken across the boundaries where two α' plates met (Fig. 2a). In every case the patterns so obtained could be indexed either as an exact or a close matrix/{1 0 $\bar{1}$ 1} twin relationship (Fig. 2b).

The dislocation density of the martensite increases slightly with silicon content; however, the same two types of dislocation were observed in all of the alloys although the second type was not observed in the unalloyed titanium:
(i) random arrays of dislocations (Fig. 3)
(ii) arrays of straight dislocations lying in the $\langle 11\bar{2}0\rangle$ directions (Fig. 4). Visibility criteria for these dislocations were established using two beam darkfield microscopy.

$\mathbf{g}$ = (0002)	{10$\bar{1}$0}	{10$\bar{1}$1}	{11$\bar{2}$0}
Type (i) I	V	V	V
Type (ii) V	I	V	I

The notation I indicates that the dislocation gave very weak or zero contrast when imaged under any specific variant of the indicated type of reflection $\mathbf{g}$. V indicates that the dislocation could be imaged under some variants of the indicated reflection. These results are consistent with type (i) being $\frac{1}{3}\langle 11\bar{2}0\rangle$ dislocations and type (ii) [0001], the absence of contrast using {11$\bar{2}$0} reflections eliminating the $\frac{1}{3}\langle 11\bar{2}3\rangle$ vector. It should be noted, however, that the degree of specimen tilting available did not permit the same dislocations to be imaged using (0002) and both {10$\bar{1}$0} and {11$\bar{2}$0}. Both sets are shown to be genuine defects of the martensite and not introduced during thinning since specimens aged as bulk material exhibit silicide precipitation upon both types of dislocations [3].

The Ti-5Zr alloy showed a structure similar to that of the Ti-1Si alloy, while the Ti-Al alloy resembled more closely the unalloyed titanium, consisting of massive martensite.

3.2. Ternary Ti-Zr-Si alloys

In all of these alloys the martensite consisted of plate shaped crystals (Fig. 5); the trend is towards increasingly fine structures with increase in either silicon or zirconium contents, e.g. Fig. 1d.

In the alloy of highest zirconium content (Ti-10Zr-1Si) the martensite crystals are a factor of 100 times smaller than in the previously mentioned alloys (Fig. 6). Large numbers of silicide particles were present which had not been take into solution at 1200°C and the β grain size was finer; no retained β was detected.

As in the binary alloys, $\frac{1}{3}\langle 11\bar{2}0\rangle$ and [0001] dislocations and twin related martensite plates were observed. Higher than average densities of $\frac{1}{3}\langle 11\bar{2}0\rangle$ dislocations were observed near the point of impingement of secondary plates upon primary plates and stacking faults were frequently observed. Trace analysis indicated that the faults

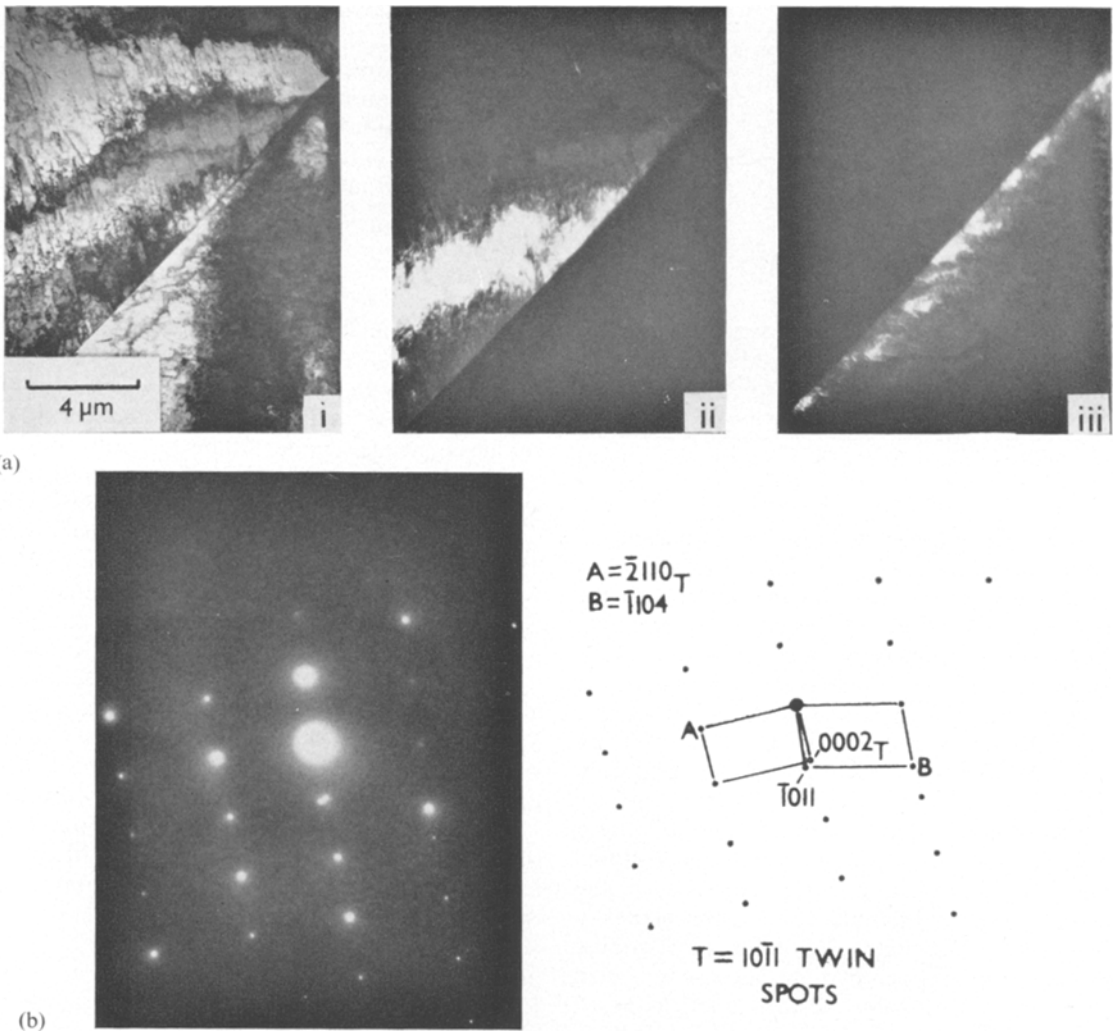

Figure 2 (a) (i) Bright field). (ii) Low resolution darkfield, (spot A) (iii) low resolution dark field (spot B) Ti-1Si. ST 1200°C/24 h WQ. Two twin-related martensite plates.
(b) Selected area diffraction pattern of Fig. 2(a) and key.

lie in the basal plane and they exhibit visibility criteria consistent with a $\frac{1}{3}\langle 10\bar{1}0\rangle$ fault vector. $\{10\bar{1}1\}$ twins were infrequently observed within the martensite plates.

3.3. Alloys containing aluminium and silicon

The structure of the Ti-5Al-1Si alloy is a mixture of massive martensite colonies and larger parallel sided plates. In the alloy series based on Ti-5Zr-1Si, additions of aluminium produce a more regular martensite, the size difference between the largest and smallest plates with regard to both length and width, being reduced e.g. cf Figs. 1d and e. The substructure of the martensite in all of these alloys is similar to that of the Ti-Si and Ti-Zr-Si alloys although the martensite plates sandwiched between the larger plates are generally "block like" rather than platelike or lenticular. Aluminium additions also tend to reduce the β grain size.

3.4. IMI 685 type alloy

The martensite in the IMI 685 type alloy (the commercial alloy contains only 0.25% Si, nominal, but is otherwise similar to the experimental alloy) consists essentially of colonies of

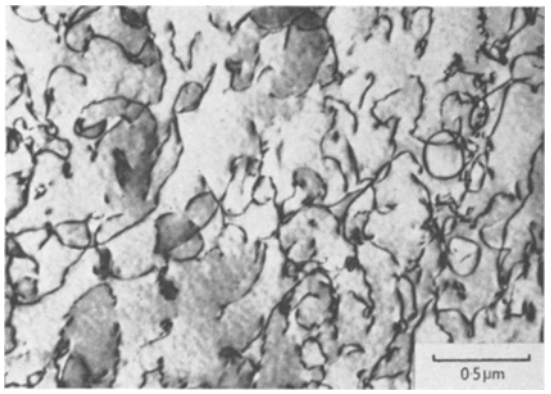

Figure 3 Ti-1Si $\frac{1}{3}\langle 11\bar{2}0\rangle$ dislocations within a large martensite plate.

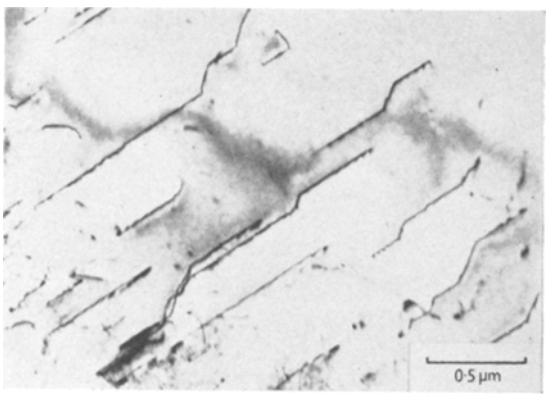

Figure 4 Ti-1Si. c[0001] dislocations within a large martensite plate g = (0002).

plates of parallel orientation together with larger plates of differing orientation (Fig. 1f) but the boundaries show a distinct contrast which results in their appearing thick and dark (Fig. 7). Since the misorientation across the sub-boundaries is small, essentially single-crystal selected-area diffraction patterns could be obtained from are as containing many sub-boundaries. Extra spots observed in the diffraction patterns were found to be produced by the dark sub-boundaries and could be indexed in terms of the bcc β-phase. The orientation relationship between the α' and β phases was in all cases a variant of Burgers relationship:

$$(0001)\,\alpha' \,//\, (011)\,\beta$$
$$[\bar{1}2\bar{1}0]\,\alpha' \,//\, [\bar{1}\bar{1}1]\,\beta$$

Re-solution treatment at 1050°C for 1 h, i.e. the temperature used in commercial practice [2]

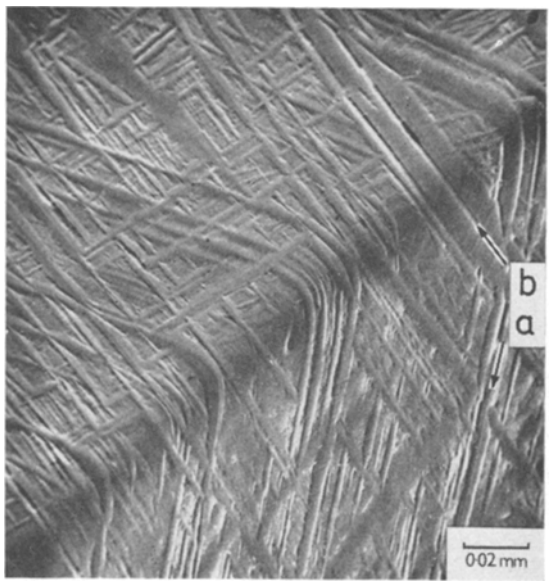

Figure 5 A scanning electron micrograph of two orthogonal surfaces of a martensitic specimen of Ti-5Zr-1Si illustrating the plate structure of the martensite. The arrows indicate (a) light-etching and (b) dark-etching midribs.

reduced the martensite plate size by a factor of two, but the hardness increased by only 12 VPN.

3.5. The martensite midrib

Light microscopical examination of the alloys showed that many of the martensite plates exhibit an extremely straight linear feature running down the plate centre and along its entire length. Two distinct types of such "mid-rib" are observed, one more deeply etched and the other less deeply etched than the surrounding material (e.g. Figs. 1 and 5). The dark-etching midrib consisted of small regions of finely transformed material sandwiched between plates of similar orientation (Fig. 8).

The nature of the light-etching midrib is more difficult to determine. In many martensite plates a band of dislocation free material was observed running down the centre of the martensite plates. This is seen most easily in Ti-5Zr-5Al-1Si after ageing to produce silicide precipitates on the dislocations which can, as a result of this decoration, be observed under any operating reflection (Fig. 9). This feature, although common, is only consistently observed in the aluminium-containing alloys.

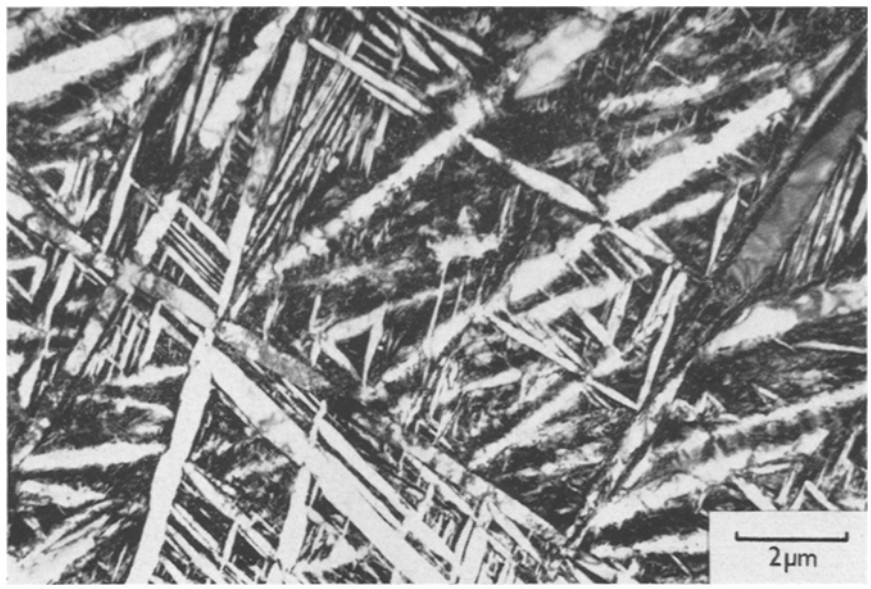

Figure 6 Ti-10Zr-1Si. 100% α' structure consisting of fine martensite plates.

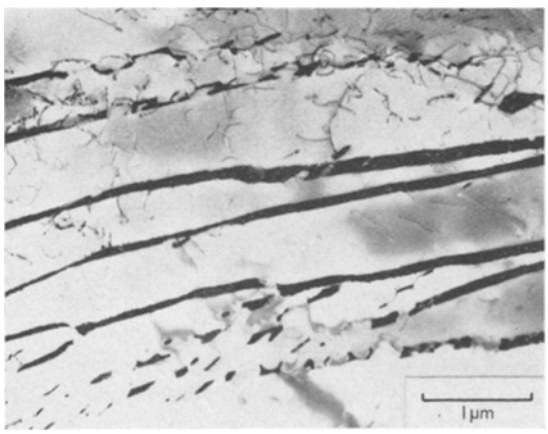

Figure 7 IMI 685 type alloy. Sub-boundaries in the martensite containing retained β.

3.6. Martensite strength

The strength of the martensite was determined by hardness measurement of sections of the quenched specimens. The hardness results are presented in Fig. 10. The binary alloy data show that silicon is the most potent strengthening agent, zirconium the next most effective while aluminium is the least effective in terms of atomic percent.

4. Discussion

4.1. Structure of martensite

4.1.1. Morphology

The main aspect of interest concerning the martensite morphology is the relationship between alloy composition and the size, shape and distribution of the crystals. The progression from massive to plate-like and lenticular martensite observed in the binary titanium-silicon system with increase in solute content resembles that reported in the titanium-copper system [7]. There is an interesting comparison with the transition from massive to plate-like martensite in Fe-Ni and Fe-C alloys occurring with increase in solute and decrease in M_s and associated with a change in the martensite habit and sub-structure. Magee and Davies [8] have interpreted this transition in terms of the flow strength of austenite and martensite, suggesting that martensite forms with a habit plane requiring the least plastic work.

The morphological transition in titanium alloys is probably associated with the effect of alloying on the strength of the α- and β-phases. Silicon is the most effective in promoting the transition, with zirconium next and aluminium the least effective: this is also the order of effectiveness in producing solid solution

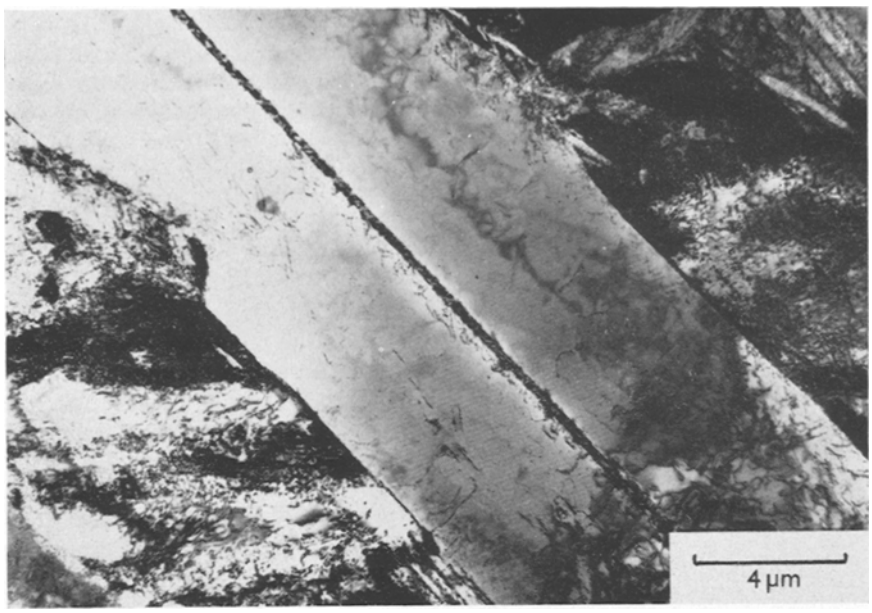

Figure 8 A martensite midrib consisting of a band of finely transformed β within a large martensite plate.

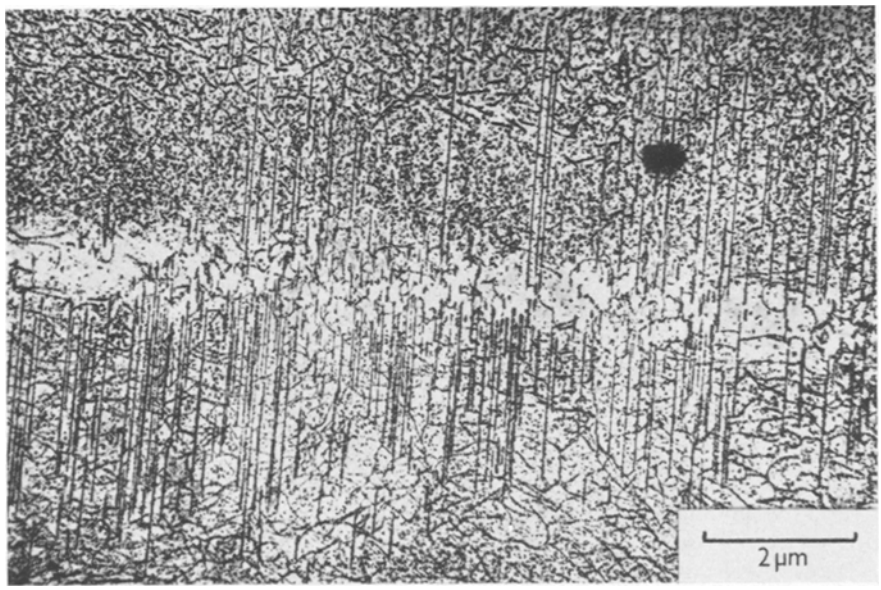

Figure 9 Ti-5Zr-5Al-1Si aged 550° C/13 weeks. Dislocation decoration by silicide precipitates reveals a band of low dislocation density running along the centre of a martensite plate.

strengthening in the martensite. It is reasonable to assume that the same order is followed for solid-solution strengthening of the β-phase.

Garwood [9] has suggested that massive martensite is produced when slip deformation in the region of the martensite/austenite interface reduces the stress field in the austenite produced by the martensite plate. This permits a second plate to form adjacent to the first with the same variant of the orientation relationship and habit plane; repetition of this process thus produces a massive martensite colony. Magee [8] assumes

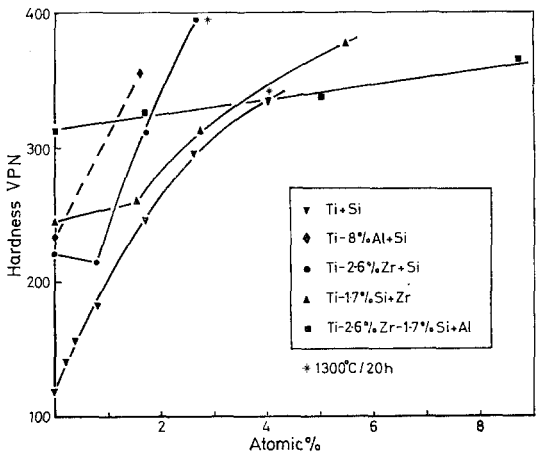

Figure 10 The hardness of martensite in the Ti-Zr-Al-Si system after solution treatment at 1200° C for 24 h.

that in ferrous massive martensites, slip in both austenite and martensite is required for this process. Strengthening by solute in solid solution will inhibit the accommodation slip process and thus prevent the growth of a second plate next to the first on the same habit. In ferrous systems inhibition of slip in the martensite may lead to twinning of the martensite and hence a change in habit plane as in the morphology. Very little twinning has been observed in the present work and it may be assumed that the solid-solution strengthening only inhibits the accommodation slip. Thus, in soft β the bulk stress field in a grain may promote a limited number of martensite variants preferentially and, as a result of accommodation slip, these can form large massive martensite colonies, each filling a large part of the β grain. In hard β the stress field of the first martensite plates inhibits the growth of similar plates in close proximity to them. In the regions of β partitioned by these plates other variants may nucleate, again certain variants being preferred because of the local stress field. Thus a conventional plate type martensite is produced. At intermediate strength levels mixed structures containing both conventional plates and massive colonies may be observed (e.g. Ti-1Si Fig. 1b).

In the present work it appears that individual members of the massive colonies have the same habit as the more conventional martensite plates. This is consistent with previous work on titanium alloys. A change to a $\{344\}\beta$ habit only occurs in highly β stabilized alloys and has been shown by Hammond and Kelly [10] to be associated with internal twinning of the martensite plates.

Differences in plate width between the various alloys (e.g. aluminium containing alloys show the widest plates) may result from the occurrence of an isothermal component in the martensite transformation, varying in extent with the individual alloy additions.

4.1.2. Substructure

The observation of $\frac{1}{3}\langle 11\bar{2}0\rangle$ dislocations in the martensite is consistent with the results of other workers in other titanium alloys, e.g. [7]. The higher-than-average dislocation densities observed at martensite plate intersections suggest that stress concentration due to the secondary plate causes deformation of the primary plate.

[0001] dislocations have not been identified in titanium alloy martensites previously, although Nishiyama *et al* [5] suggested that linear features observed in the $\langle 11\bar{2}0\rangle$ directions in martensitic commercial purity titanium were dislocations. From the precise alignment of dislocations in the martensite it appears possible that they are debris left by the advancing martensite interface. Williams *et al* [7] have observed $\frac{1}{3}\langle 11\bar{2}3\rangle$ dislocations in the sub-boundaries in massive titanium-copper martensites and suggest that these produce the lattice invariant shear, this result being consistent with the theoretical prediction of Crocker [11] and Otte [12]. It is possible that the intersection of $\frac{1}{3}\langle 11\bar{2}3\rangle$ dislocations on $\{10\bar{1}1\}$ planes with suitable dislocations at the β/α interface could produce the observed [0001] dislocations lying along the line of intersection of the two slip planes.

The $\frac{1}{3}\langle 10\bar{1}0\rangle$ stacking faults have previously been observed by a number of workers in a variety of titanium alloys (e.g. [13]) and would thus appear to be a general feature of titanium alloy martensites. Similarly, the $\{10\bar{1}1\}$ internal twins have been observed previously in other systems [10].

Occasional $\{10\bar{1}1\}$ twin relationships between individual martensite plates have been reported previously [7, 14, 15]. Such relationships were found in this work to be very common. However, diffraction patterns containing spots from two variants with a common $\langle 11\bar{2}0\rangle$ zone axis contained 0001 directions at $59 \pm 1°$ to each other compared with $\sim 57\frac{1}{2}°$ expected from an exact twin relationship. It is possible that such apparently twin-related variants could simply be

two specific Burgers variants: e.g. the two variants

$$(0001)_{\alpha 1} // (\bar{1}01)_{\beta}\ (0001)_{\alpha 2} // (011)_{\beta}$$
$$[2\bar{1}\bar{1}0]_{\alpha 1,\ \alpha 2} // [1\bar{1}1]_{\beta}$$

contain a common $[2\bar{1}\bar{1}0]$ direction at right angles to the two (0001) planes which in turn are at 60° to each other. A rotation of one of the variants by less than 3° (the exact value depending on the c/a ratio) about the common $[2\bar{1}\bar{1}0]$ axis reducing the angle between the two (0001) poles produces an exact $(01\bar{1}1)$ twin relationship between the two variants. The observations indicate that the Burgers relationship better describes the facts than a twin relationship. The lattice invariant shear could produce the deviation from the exact Burgers relationship. Also a genuine twin relationship, although possibly reducing the elastic strain of the nucleation, could not reduce the strain involved in the growth of the martensite to produce a {334} habit plane (known to be typical of titanium alloys not containing significant quantities of β-stabilizing elements) and the co-operative growth of twin-related variants would not be expected. The Burgers relationship predicts 12 possible α' variants for each original β grain and if these occurred at random, $\frac{1}{3}$ of the observed martensite plates would appear approximately $\{10\bar{1}1\}$ twin-related. The frequency of observed near twin-relationships indicates that such pairs of martensite plates may nucleate cooperatively. The similarity between twin- and Burgers-related variants has previously been noted by Otsuka and Shimizu in Cu-Al-Ni alloy martensites [16].

4.1.3. Midribs

The dark etching type of midrib consists of finely transformed material sandwiched between plates of parallel orientation, these parallel plates being nucleated separately. In some cases, however, it appears that the midrib forms when a single plate splits into two parts, the midrib starting as a sub-boundary and broadening into the band of finely transformed material, e.g. in the IMI 685 type alloy some of the β-containing sub-boundaries started within a single martensite plate and divided it into two or more parts. The light midrib which appears to consist of a region of low defect density presumably represents the thin region where the transformation originated, dislocation debris being left as the martensite interface advances. Williams *et al* [7] have suggested that after the initial shear plate is formed the interface advances with $\frac{1}{3}\langle 11\bar{2}3\rangle$ dislocations providing the lattice invariant shear and that as plate thickening continues a second shear system operates involving $\frac{1}{3}\langle 11\bar{2}0\rangle$ dislocations; this might increase the amount of debris produced and increase the difference in dislocation content between the centre and edge of the martensite plate.

4.1.4. Retained β-phase

The thin layers of β phase in the IMI 685 type alloy resemble those reported in a Ti-6Al-5Sn-2Zr-0.8Mo-0.25Si alloy [17] and in Ti-Mo-Si alloys [18]. From work on the latter alloys it appears that the β-phase becomes enriched in molybdenum by diffusion during quenching and a small proportion of this phase is retained.

4.2. Strength

The present results do not provide a basis for a quantitative analysis of the strengthening contributions in the martensite, but some features are worthy of note.

From the values of 0.1% proof stress found for recrystallized α in the Ti-5Zr alloy ($\sim$ 550 MNm^{-2}) as compared with that for the martensitic α' ($\sim$ 625MNm^{-2}) it appears that the contribution of solid-solution strengthening is dominant. The contribution of dislocation density should be similar for all the alloys. The effect of α' plate size will vary from one alloy to another (e.g. compare the fine structure of α' in the Ti-Zr-Si with that in Ti-Si). Concerning solid-solution strength the effectiveness of the alloying elements as strengthening agents in the binary alloys decreases in the sequence silicon, zirconium and aluminium, reflecting the decreasing differences in atomic diameter of these elements with respect to titanium. The effect of several alloying elements in combination is clearly complex: for example the sum of the separate hardening effects of 8.5 at. % Al and 1.7 at. % Si (265 VPN) is almost identical to their effects in combination while 0.75 at. % Si and 2.6 at. % Zr produce in combination roughly the same amount of hardening (100 VPN) produced by 2.6 at. % Zr alone, in spite of the fact that the ternary Ti-Zr-Si alloy exhibits a finer martensite than the binary alloy containing zirconium. These results suggest that there is a positive interaction between zirconium and silicon. The silicon atom is 21% smaller than the titanium atom while the zirconium atom is 9%

larger and there is evidence that these elements form clusters, which may reduce the lattice strain and thus reduce the solid-solution strengthening. Such an effect is, however, limited to small alloying additions since, as shown in Fig. 10, after the initial slight hardening upon adding both silicon and zirconium to titanium increased additions produce marked strengthening. Indeed additions of more than 1 at. % silicon to Ti 2.6 at. % Zr produced greater hardening than that shown by binary titanium-silicon alloys. Further work is needed to analyse fully the strength of titanium alloy martensites.

5. Conclusions

(1) The martensite in the titanium-silicon system changes from massive colonies of α' plates to structures containing individual plates occurring with different variants of the habit plane; this transition occurs over a range of only 0 to 4 at. % silicon. In the ternary and more complex alloys, e.g. Ti-Zr-Si and Ti-Zr-Al-Si there is a similar trend to plate-like structures with increasing solute content. This is not accompanied by a change in the shear mechanism.

(2) [0001] and $\frac{1}{3}\langle 11\bar{2}0\rangle$ dislocations, and $\frac{1}{3}\langle 10\bar{1}0\rangle$ stacking faults are common features of titanium martensites in near-α alloys of the Ti-Zr-Al-Mo-Si system. The transformation follows approximately the Burgers relationship and produces near $\{10\bar{1}1\}$ twin-related martensite plates.

(3) Martensite midribs are a feature of titanium alloy martensites and consist of finely transformed material or of a region of low defect density.

(4) The presence of only 0.5% molybdenum results in the retention of thin layers of β-phase at the martensite plate boundaries in the IMI 685 type alloy.

(5) The strength of martensites in the Ti-Zr-Al-Mo-Si system is determined primarily by solid solution strengthening, involving complex interactions between the various types of solute atoms.

Acknowledgements

Acknowledgement is made to Imperial Metals Industries (Kynoch) Ltd and the General Electric Company for the donation of materials, to the Science Research Council for the provision of a grant to one of the authors (H. M. Flower) and to Professor J. G. Ball for the provision of laboratory facilities.

References

1. M. KATCHER, *Metals Eng. Quart.* August **19** (1968).
2. *Metal Progress.* Titanium Alloy Data Sheet, **95** (3) (1969).
3. H. M. FLOWER, P. R. SWANN, and D. R. F. WEST, *Met. Trans.* **2** (1971) 3289.
4. A. D. MCQUILLAN and M. K. MCQUILLAN, "Titanium" (Butterworths Scientific Press, London, 1956).
5. Z. NISHIYAMA, M. OKA, and H. NAKAGAWA, *Trans. Jap. Inst. Metals*, **7** (1966) 168.
6. R. H. ERICKSEN, R. TAGGART, and D. H. POLONIS, *Acta Metallurgica*, **17** (1969) 553.
7. J. C. WILLIAMS, R. TAGGART, and D. H. POLONIS, *Met. Trans.* **1** (1970) 2265.
8. C. L. MAGEE and R. G. DAVIES, *Met. Trans.* **2** (1971) 1939.
9. R. D. GARWOOD, "Martensite," ed. E. R. Petty (Longman, London, 1970) 107.
10. C. HAMMOND and P. M. KELLY, *Acta Metallurgica* **17** (1969) 869.
11. A. G. CROCKER, Ph.D. Thesis, University of Sheffield (1959).
12. H. M. OTTE, "The Science, Technology and Application of Titanium" (Pergamon Press, London, 1970) 645.
13. J. C. WILLIAMS and M. J. BLACKBURN, *Trans. ASM* **60** (1967) 373.
14. Z. NISHIYAMA, S. SATO, M. OKA, and H. NAKAGAWA, *Trans. Jap. Inst. Metals*, **8** (1967) 127.
15. T. YAMENE and J. UEDA, *Acta Metallurgica*, **14** (1966) 438.
16. K. OTSUKA and K. SHIMIZU, *Jap. J. Appl. Physics*, **8** (1969) 1196.
17. S. R. SEAGLE and H. B. BOMBERGER, "The Science, Technology and Application of Titanium" (Pergamon Press, London, 1970) 1001.
18. R. G. NICHOLS, unpublished work.

Received 4 January and accepted 10 February 1972.